

The shape of the contact-density function matters when modelling disease transmission in fluctuating populations

Benny Borremans^{1,2,3*}, Jonas Reijnders^{1,4}, Niel Hens^{3,5}, Herwig Leirs¹

¹ Evolutionary Ecology Group, University of Antwerp, Belgium

² Department of Ecology and Evolutionary Biology, University of California Los Angeles, United States

³ Interuniversity Institute for Biostatistics and statistical Bioinformatics (I-BIOSTAT), Hasselt University, Belgium

⁴ Department of Engineering Management, University of Antwerp, Belgium

⁵ Centre for Health Economics Research & Modelling Infectious Diseases (CHERMID – VAXINFECTIO), University of Antwerp, Belgium

*correspondence: bennyborremans@gmail.com

Keywords

Contact rates; Herd immunity; Invasion; Mass action; Nonlinearity; Threshold

Important notice

This is a pre-print version of the manuscript, made available through bioRxiv.org. Note that this manuscript has not yet been peer-reviewed, and has been submitted to a peer-reviewed journal.

Abstract

Models of disease transmission in a population with varying densities must assume a relation between infectious contacts and density. Typically, a choice is made between a constant (frequency-dependence) and a linear (density-dependence) contact-density function, but it is becoming increasingly clear that nonlinear functions intermediate between these two extremes are more realistic. It is currently not clear however what the consequences would be of implementing different contact-density functions when population density varies. By combining existing data on *Mastomys natalensis* demography, density-dependent changes in contacts, and Morogoro virus infection dynamics, we explored the effects of different contact-density function shapes on transmission dynamics and invasion/persistence. While invasion and persistence were clearly affected by the shape of the function, the effects on outbreak characteristics such as prevalence and outbreak size were minor. As a consequence, it would be difficult to distinguish between the different shapes based on how well models fit to real data. This data-driven study confirms that the shape of the transmission-density function must be chosen with care, ideally based on existing information such as a previously quantified contact- or transmission-density relationship or the underlying biology of the host species in relation to the infectious agent.

Introduction

The transmission of infections can be sensitive to changes in population density, especially in the case of fluctuating wildlife populations [1–3]. When modelling disease transmission, the probability of encountering an infected individual is typically assumed to be either independent of (frequency-dependent) or linearly dependent on (density-dependent) population density [4]. Sexually transmitted infections are generally described using frequency-dependent transmission because the number of sexual contacts is assumed to remain constant, regardless of population density [5], while infections that are transmitted through regular “every-day” contacts are often assumed to be density-dependent [6].

The choice of which contact-density function to use in a model of disease transmission must be made with care because it entails potentially significant consequences. Most importantly, the functions differ in whether or not an infection is expected to persist below a critical density of individuals [7]. The basic reproductive number (R_0), defined as the number of secondary infections arising from the introduction of one infectious individual entering a completely susceptible population, is a central epidemiological measure that characterises the spread of an infection, as it

provides an immediate approximation as to how rapidly an infection can spread [8]. In its simplest form, $R_0 = \beta N$, where N is population size and β is the transmission coefficient that consists of the rate p of becoming infected through contact with an infectious individual, multiplied by the contact-density function that equals cN/A (where A is area) when linear (density-dependent) and c when constant (frequency-dependent), and random homogenous mixing is assumed [9]. When the transmission coefficient β changes with density, theory predicts a density below which the transmission rate is too low, causing R_0 to fall below 1 and the disease to disappear, whereas no persistence threshold density exists when β remains constant, independent of density [1,10,11]. Because changes in the transmission coefficient determine how quickly an infection can spread through a population, it can also be expected that the two contact-density functions will differently affect outbreak characteristics such as incidence, prevalence and outbreak size [12].

Because human populations are usually large and stable, many models of human disease transmission are not significantly affected by the choice of the contact-density function, which may explain why the consequences of the shape of different contact-density functions have been little explored. But when one is interested in describing or predicting infection dynamics in populations of different sizes, at low densities, or with periodically fluctuating densities, the shape of the assumed contact-density function may become highly important [3]. Although in human populations we can expect a role of the assumed contact-density function in situations determined by the interplay between the timescales of demographic transition and epidemic evolution (e.g. high disease-related mortality), such situations are most common for wildlife infections, so it is not surprising that studies on how transmission rates and contacts relate to density have mainly been conducted in this field [9,13–17]. The main approach in these studies has been to measure transmission in a field or experimental setting in which densities are manipulated or vary naturally, which is then followed by creating a mathematical model of transmission to test which transmission-density function results in a better fit of the model to data.

There has traditionally existed a focus on whether transmission is frequency- or density-dependent, and rarely have other, nonlinear transmission-density functions been investigated. For example, a study in which densities of the two-spot ladybird (*Adalia bipunctata*) were manipulated and transmission of sexually transmitted parasitic mite *Coccipolipus hippodamiae* was measured, only tested whether the transmission-density relationship was density-dependent or not, even though their results strongly suggest that the relationship more closely resembles a nonlinear asymptotic power function [18]. Similarly, a recent study in which strong emphasis was put on estimating a persistence threshold for Sin Nombre virus transmission in deer mice, assumed linear density-

dependence without further investigation, although other transmission-density functions may have significantly altered model results [19].

Nevertheless it has been well established that the binary distinction between density-independence or linearity can be inadequate, and a range of other possible nonlinear transmission functions has been suggested, often in the power law, asymptotic or logistic family [9,20–22]. Cowpox virus dynamics in a natural population of field voles (*Microtus agrestis*) for example has been shown to be best described by a nonlinear power function that is intermediate between density independence and linearity [13]. Intermediate density-dependence was also observed in *Ambystoma tigrinum* virus transmission in the tiger salamander [20].

Here, we want to investigate whether, and in which situations, implementation of the exact shape of the transmission response function is important. Although it would be possible to mathematically model the effects of different transmission-density functions for any hypothetical combination of demographic pattern and contact-density function, the sheer number of possible functions for each demographic situation would make it almost impossible to decide which functions are biologically relevant. To inform such models we therefore need biological background data, i.e. a species for which population dynamics, a contact-density function, and disease dynamics have been quantified, but until recently no such data were available. Using a combination of data from recent experiments in which we quantified contact rates across a wide range of population densities in the rodent *Mastomys natalensis* [23] and the infection parameters of Morogoro virus (MORV) in this rodent [24], we tested the effect of different transmission functions using a simple SIR transmission model in annually fluctuating host populations. By implementing a range of hypothetical combinations of infectious period, transmission rate and population size, we assessed what the effects of the contact-density would be for infections with different characteristics.

Materials and methods

Background data

Natal multimammate mice (*Mastomys natalensis*) occur throughout Sub-Saharan Africa, and are an important agricultural pest species and natural reservoir hosts for several microparasites that cause disease in humans, including *Yersinia pestis* (bubonic plague), leptospirosis and several arenaviruses including Lassa virus, which can cause severe haemorrhagic fever in humans [25–29]. Its demography has been studied thoroughly, which allows us to create a simple but accurate demographic model that will serve as a basis for transmission modelling (see below). In Tanzania, where most of the studies on its population ecology have been conducted, *M. natalensis* exhibits

strong annual population fluctuations, with densities ranging from 10/ha in the breeding season to > 300/ha in the non-breeding season [30,31]. Importantly, we have recently quantified the contact-density relationship for this species, which provides us with a realistic biological background for fitting the transmission functions [23].

The simulated infection dynamics in this study are based on those of Morogoro arenavirus (MORV), which naturally occurs in *M. natalensis* in Tanzania, and of which the transmission ecology [32] and patterns of infectivity [24] have been documented in detail; it has a latent period of about 3 days between infection and excretion (which we here ignored for simplicity), an infectious period of 30-40 days, and presumably lifelong immunity. MORV transmission can therefore be modelled using a simple SIR model (described below).

Study design – models

We investigated the effect of four different contact-density functions on simulated MORV transmission. Prevalence and incidence patterns were examined using a deterministic model because we do not want to assess the effect of random fluctuations on these parameters, while invasion and persistence were investigated using a stochastic model because these two parameters are per definition determined by random events, as explained below.

Demographic model

The seasonally fluctuating densities of *M. natalensis* were modelled using a seasonal birth-pulse function, $B(t) = k \exp[-s \cos^2(\pi t - \varphi)]$, as described in Peel *et al.* [33]. This is a flexible function in which a synchrony parameter (s) determines the length of the birth period, and another parameter (φ) determines the timing of the birth period. Parameter k ensures that the annual population size remains the same, by compensating the number of births for the (constant) mortality rate μ [33]. Function parameters were fitted visually to a 20-year dataset of monthly population densities of *M. natalensis* in Tanzania ([30,31] and more recent unpublished data; Appendix Figure S1-1). This deterministic demography was also used as a basis for modelling demography in the stochastic SIR model (described below) in order to avoid the influence of stochastic changes in population density. Because deterministic demography results in non-integer (rational) changes in the number of births and deaths while the stochastic SIR model is based on events and births/deaths must therefore be integers, the demographic model was adapted slightly by rounding the total numbers of births and deaths in each 12h interval and adding the remainder to the next event.

Transmission model

A standard SIR (Susceptible, Infectious, Recovered) model was used to simulate MORV transmission [34,35]. The deterministic version of this model is given by the following set of coupled ordinary differential equations:

$$\frac{dS}{dt} = B(t)N - \beta S \frac{I}{N} - \mu S$$

$$\frac{dI}{dt} = \beta S \frac{I}{N} - \gamma I - \mu I$$

$$\frac{dR}{dt} = \gamma I - \mu R$$

where $B(t)$ is the time-dependent birth function described earlier, μ represents the mortality rate, γ is 1/infectious period, and $\beta = cp$ is the transmission coefficient, which is composed of p (rate at which S becomes I when in contact with an I individual) and contact-density function $c(\frac{N}{A})$ that can acquire different shapes depending on population density (explained below).

For comparing the infection invasion and persistence probabilities between different contact-density functions, we used a stochastic discrete time version of the SIR model, where the transition rates between categories were modelled stochastically, resulting in two possible stochastic events: infection (decrease of S, increase of I) and recovery (decrease of I, increase of R). Events were assumed to occur continuously in time at a certain rate, and were modelled using the “adaptive tau-leap” algorithm described in [33,36]. Briefly, each short time-step δt , the number of events of each type that occurs is randomly drawn from a Poisson distribution with mean $r_i \delta t$, where r_i is the rate of each type of event i . If the number of simulated events would cause any of the categories (S, I or R) to fall below 0, δt is halved and new events are drawn (= “adaptive tau-leap”).

The model started at $t = 0$ and one infected individual was introduced after one year, at $t_0 = 1$ ($I \rightarrow 1$) in order to allow the initial population dynamics to stabilise. Different introduction times only had an effect on the linear and sigmoid functions, where they resulted in lower invasion probabilities between t_0 values of 1.2 and 1.4, which was likely a result of the low population densities (Appendix Figure S2-1). There was no effect of introduction time on disease persistence (Appendix Figure S2-2).

Four different contact-density functions

The core of this study is the implementation of four different, biologically relevant contact-density functions $c = f(\frac{N}{A})$ (Fig. 1):

- (a) Constant function (or “frequency-dependence”) $c = a_1 (\frac{N}{A})^0$, with fitting parameter a_1 . Independent of density, and typically (but not only) used in the case of sexually transmitted

infections where the number of sexual contacts is not expected to change with population density [5,7].

(b) Linear function (or “density-dependence”) $c = a_2 \left(\frac{N}{A}\right)$, with fitting parameter a_2 . Typically used when assuming random mixing where (infectious) contacts increase linearly with population density [35,37].

(c) Power function $c = a_3 \left(\frac{N}{A}\right)^{a_4}$, with fitting parameters a_3 and a_4 . Has been used as an “intermediate” between frequency- and density-dependence [9,20]. Contact rates increase almost linearly at low densities, but the slope decreases at higher densities towards an asymptotic limit. This shape has been observed for contact rates in brushtail possums and elk [38–40], and has been shown to be a better predictor of cowpox transmission patterns than either frequency- or density-dependence [13].

(d) Sigmoid function $c = a_5 / (1 + e^{a_6 \left(\frac{N}{A}\right)^{-a_7}})$ with fitting parameters a_5 , a_6 and a_7 . This function has a minimum, constant number of contacts at low densities, after which contact rates increase almost linearly with density until reaching a plateau when reaching a maximum number of contacts. This shape has been observed for multimammate mice contacts [23], and has been proposed previously as a biologically plausible function [9].

These four different functions could in theory acquire an infinite number of shapes, so in order to realistically model these four functions, they were fitted to empirical contact-density data of *M. natalensis* [23] using a maximum likelihood approach.

Fitting transmission coefficient β

Considering that $\beta = cp$, after fitting contact parameter $c\left(\frac{N}{A}\right)$ to contact-density data for the four functions, a transmission rate p had to be determined before being able to compare the effect of the different transmission-density functions. Equivalent to fitting model parameters to data, a function-specific constant (q_i) had to be fitted for each function i to a common characteristic. Out of numerous possible characteristics to choose for fitting, we opted for one that ensured that β , summed across the probability distribution of population densities occurring during one year in a simulated, deterministic model of demography, was the same for each contact function. Formally, this meant that: $\beta = q_i \times \sum_{j=1}^{300} f_c\left(\frac{N}{A}\right)_j \times h\left(\frac{N}{A}\right)_j$, where f_c is the contact-density function, j is population density and h is the frequency distribution of densities in a year. We chose this method because it has the advantage of not selecting for certain outbreak characteristics such as prevalence or outbreak size. We nevertheless also examined the effect of using two different fitting methods;

one that fitted q_i so that the deterministic transmission models resulted in a maximum annual prevalence of 40%, and one where q_i was fitted so that the final annual number of infections was $2N_0$, i.e. twice (an arbitrarily chosen number) the initial number of individuals). While these different fitting methods resulted in highly different values for the constant function, the three other functions were always very similar (Appendix Table S3-1 and Figure S3-1). As we are mainly interested in the differences between the three non-constant functions, we did not further investigate these effects using the two other β -fitting methods.

Statistics

The effects of the contact-density functions were investigated through a number of meaningful epidemiological parameters: (1) SIR dynamics; (2) Incidence ($\beta S \frac{I}{N}$); (3) Prevalence ($\frac{I}{N}$); (4) Invasion probability, defined as the proportion of stochastic simulations in which the infection manages to survive the first year after introduction, conditional on having started successfully (successful start = infection persistence time $> t_0$ + infectious period); (5) Persistence probability, defined as the proportion of stochastic simulations in which, conditional on having survived the first year, the infection is still present at $t = 10$ years. The first three parameters were investigated using deterministic models, while the latter two were calculated using stochastic simulations.

Invasion and persistence were estimated under a number of conditions of population size (N_0), infectious period ($\frac{1}{\gamma}$) and transmission rate (p), where for each combination of these conditions 1,000 simulations were run. While we model changes in population *density* for each combination of parameters, we also assess the effect of population *size* because this is expected to affect the probability for the infection to disappear from the population, independent of density. In order to ensure that we here implemented the effects of population size and not density, population density $\frac{N}{A}$ was calculated assuming that the area occupied when initial population size $N_0 = 100$ is 1 ha, and that area increases linearly with increasing values of N_0 (i.e. when initial population size increases, area also increases).

Results

Deterministic models

Because we are interested in the broad qualitative effects of the contact-density functions rather than in detailed differences that are more likely to be specific to the model system, we here report the results qualitatively. The constant function resulted in a relatively low epidemic peak during the breeding season, while the other three functions (and especially the sigmoid function) showed

similar patterns with a clear epidemic peak (Figure 2). Incidence ($\beta S \frac{I}{N}$) and prevalence ($\frac{I}{N}$) were spread evenly across the year for the constant function, while the epidemic peak observed for the other three functions coincided with a concentrated pulse in both incidence and prevalence (Figure 3). The sigmoid function resulted in a slightly later but steeper incidence increase, and a higher maximum incidence (Figure 3a). Prevalence was similar for the three non-constant functions (Figure 3b).

Invasion and persistence

Using a stochastic version of the deterministic SIR models, invasion and persistence probabilities were investigated for a range of population sizes (N_0), infectious periods ($1/\gamma$) and transmission probabilities (p). Note that while infectious period results are reported in absolute days, they should be interpreted in relation to the demographic timescale used in the simulations (e.g. annual breeding, brief recruitment period), as this will aid comparison with other pathogen-host systems in which host densities fluctuate [33].

Successful invasion and persistence were more often observed for the constant function than for the other functions. While the invasion and persistence probabilities for the linear and power functions were intermediate and quite similar to each other, the sigmoid function generally resulted in low invasion and persistence success (Figures 4 and 5). For the constant function, even at low population sizes successful invasion was almost certain for infectious periods of 30 days and longer, and was even observed for an infectious period of 7 days in sufficiently large populations (Figure 4). In contrast, for the other functions successful invasion was never observed below infectious periods of 7 days, and even with an infectious period of 30 days invasion was rare for the sigmoid function. Similar patterns were observed for persistence, where the constant function resulted in the highest persistence probability while the linear and power functions had similar persistence probabilities, intermediate between those of the constant and sigmoid functions.

The effect of transmission rate on invasion and persistence was more similar between the constant, linear and power functions than that of infectious period, although the constant function still resulted in more successful invasion/persistence at lower transmission probabilities (Appendix Figures S4-1 and S4-2). The sigmoid function however was more affected by transmission probabilities than the other three functions, where for an infectious period of 30 days persistence was only possible for a combination of high transmission rate and large population size (Figure S4-2).

Invasion, but not persistence, was affected by the time of the year at which the infection was introduced (Appendix Figures S2-1 and S2-2). While this effect was weak for the constant and power functions, and intermediate for the linear function, the sigmoid function clearly resulted in a high sensitivity to the introduction time. For $t_0 = 1.2$ and $t_0 = 1.4$, which corresponds with the low-density period (Appendix Figure S1-1), invasion probability was extremely low.

Discussion

Models of disease transmission in which population densities fluctuate or are otherwise implemented cannot avoid assuming a way in which transmission scales with density [9]. We found a number of important differences between different shapes of the contact-density function. The constant (frequency-dependent) function was the most distinctive; invasion and persistence probabilities were always higher than for the other functions and were the least sensitive to low population size, infectious period or transmission rate. SIR dynamic patterns of the constant function exhibited lower and less fluctuating incidence and prevalence, with a smaller epidemic outbreak peak, than in the case of the other functions. In contrast, the patterns caused by the linear, power and sigmoid functions were similar to each other, although there were still a number of important differences. The sigmoid function gave the most pronounced incidence peak, with incidence rates that were high during but very low outside the recruitment (birthing) season. Consequently, the sigmoid function also resulted in the lowest invasion and persistence probabilities, and was the most sensitive to population size, length of the infectious period, transmission rate and timing of introduction. The linear (density-dependent) and power functions resulted in similar, less extreme incidence rates and higher invasion and persistence probabilities than the sigmoid function. Depending on the time at which the infection is introduced, the differences between the contact functions can become even more pronounced.

The different consequences of the contact-density functions can likely be attributed to a number of key differences in their shapes. Considering that the infection is most sensitive to extinction during periods of low population density, the size of transmission coefficient β at low densities will be a highly influential factor. An important consequence of this is that larger population sizes are necessary for successful disease invasion/persistence when β is low during low-density periods. In our case, for example, a minimum population size of 10,000 (equivalent to a 100ha area) was necessary for a 50% persistence success rate for the power function (30-day infectious period), while this was 50,000 for the linear function and larger than 100,000 (not tested) for the sigmoid function. Knowledge of contact rates at low population densities is therefore critical when estimating invasion and persistence thresholds.

A second important factor is the rate at which β increases with density. The maximum incidence rate and the corresponding epidemic peak will be more pronounced when there is a strong increase of β with density (e.g. the sigmoid function at intermediate densities, but also the linear and power functions). The sigmoid function for example results in a steep increase in transmission rates during the juvenile recruitment season as soon as a threshold density of susceptibles is reached (here around 80-100/ha).

When looking at SIR dynamics and invasion/persistence of the three non-constant functions, a contrast emerges that can have significant implications for fitting a β -density function to epidemiological data: while there was a clear effect of function shape on invasion and persistence, SIR dynamic patterns were quite similar. This means that it would be difficult to discern between different contact-density functions when fitting model parameters to real, inherently noisy data [3,9,13]. Nevertheless, because the functions do introduce different invasion and persistence probabilities, it will in some situations be crucial to implement the correct function. Ideally this choice is based on the quantified contact-density or transmission-density relationship of the host/infection system that is being studied, but such data are rarely available, and it would in any case not be feasible to collect these data for each infection-species combination.

A more realistic approach could be to establish general links between certain biological traits and contact and transmission patterns. The shape of the transmission-density function is determined by a combination of infection and host characteristics, so based on these characteristics, it should theoretically be possible to *a priori* predict the shape of the function. Knowledge of density-dependent changes in home range size and overlap could for example be a useful proxy for the contact-density function. For male brushtail possums (*Trichosurus vulpecula*) it has been established that contacts increase with density according to a positive power function [39], which fits with the fact that this species is not territorial, and with the observation that home ranges are larger at low densities which may result in the maintenance of contacts. Such an inverse correlation between home range size and density was also observed for *M. natalensis* [41], and this may have similar results on contact rates at low densities, as maintenance of contacts even at very low densities was also observed for this species [23]. This pattern would be expected to be different for territorial species. In an enclosure experiment, movements of meadow voles (*Microtus pennsylvanicus*), which are strongly territorial, decrease significantly with density [42], and although the effect of density on contacts was not measured, it is not unlikely that this decrease in movement distance corresponds with a contact-density function that does not increase, or at least not linearly. As a final example, consider the experimental study of the transmission of the parasitic

mite *Coccipolipus hippodamiae* in populations of the two-spot ladybird (*Adalia bipunctata*) [18]. The mite is transmitted sexually, and although sexual contacts are typically assumed to be frequency-dependent, the authors observed that the transmission-density function was closer to linear density-dependence and therefore concluded that the common assumption that sexual transmission is frequency-dependent is not always true. Their study species (*A. bipunctata*) however is known to be highly promiscuous, which means that sexual contacts are not limited to one or a few mates, but instead increase with density. *A priori* use of this knowledge about host and infection biology would have resulted in the more accurate prediction that sexual transmission of *C. hippodamiae* is density- rather than frequency-dependent.

Many wildlife species experience seasonal birth pulses and density fluctuations, and while it has been established that birth pulses can have strong effects on disease transmission [33], we now see that the shape of the transmission-density function can have further significant effects on disease invasion and persistence. The implementation of the transmission-density function should therefore be done with care, and as informed as possible. Although currently few studies have quantified the relationship between contacts and density, all relevant knowledge about host biology and behaviour can be used for deciding on the best possible shape of the transmission-density function.

Funding

This work was supported by the University of Antwerp grant number GOA BOF FFB3567, Deutsche Forschungsgemeinschaft Focus Program 1596 and the Antwerp Study Centre for Infectious Diseases (ASCID). Benny Borremans was a research fellow of Research Foundation Flanders (FWO) during the start of this study. This project has received funding from the European Union's Horizon 2020 research and innovation programme under the Marie Skłodowska-Curie grant agreement No 707840. The authors declare that no conflicts of interest exist.

Author contributions

BB, JR and HL conceived of the study; BB performed the analyses and wrote the first draft; All authors coordinated the study and helped draft the manuscript; All authors gave final approval for publication.

References

1. Anderson, R. M. & May, R. M. 1985 Vaccination and herd immunity to infectious diseases. *Nature* **318**, 323–329. (doi:10.1038/318323a0)
2. Bartlett, M. S. 1957 Measles periodicity and community size. *J. R. Stat. Soc. Ser. A* **120**, 48–70. (doi:10.2307/2342553)

3. Lloyd-Smith, J. O., Cross, P. C., Briggs, C. J., Daugherty, M., Getz, W. M., Latto, J., Sanchez, M. S., Smith, A. B. & Swei, A. 2005 Should we expect population thresholds for wildlife disease? *Trends Ecol. Evol.* **20**, 511–519. (doi:10.1016/j.tree.2005.07.004)
4. Begon, M., Bennett, M., Bowers, R. G., French, N. P., Hazel, S. M. & Turner, J. 2002 A clarification of transmission terms in host-microparasite models: numbers, densities and areas. *Epidemiol. Infect.* **129**, 147–153. (doi:10.1017/s0950268802007148)
5. Lloyd-Smith, J. O., Getz, W. M. & Westerhoff, H. 2004 Frequency-dependent incidence in models of sexually transmitted diseases: portrayal of pair-based transmission and effects of illness on contact behaviour. *Proc. R. Soc. B Biol. Sci.* **271**, 625–634. (doi:10.1098/rspb.2003.2632)
6. Van Boven, M., Koopmans, M., Van Beest Holle, M. D. R., Meijer, A., Klinkenberg, D., Donnelly, C. A. & Heesterbeek, H. 2007 Detecting emerging transmissibility of avian influenza virus in human households. *PLoS Comput. Biol.* **3**, 1394–1402. (doi:10.1371/journal.pcbi.0030145)
7. Anderson, R. M. & May, R. M. 1979 Population biology of infectious diseases: Part I. *Nature* **280**, 361–367. (doi:10.1038/280361a0)
8. Heesterbeek, J. 2002 A brief history of R_0 and a recipe for its calculation. *Acta Biotheor.* **50**, 189–204. (doi:10.1023/A:1016599411804)
9. McCallum, H., Barlow, N. & Hone, J. 2001 How should pathogen transmission be modelled? *Trends Ecol. Evol.* **16**, 295–300. (doi:10.1016/s0169-5347(01)02144-9)
10. de Jong, M. C. M., Diekmann, O. & Heesterbeek, H. 1995 How does transmission of infection depend on population size? *Publ. Newt. Inst.* **5**, 84–94.
11. Getz, W. & Pickering, J. 1983 Epidemic models: thresholds and population regulation. *Am. Nat.* **121**, 892–898. (doi:10.1086/284112)
12. Keeling, M. J. & Rohani, P. 2008 *Modeling infectious diseases in humans and animals*. Princeton and Oxford: Princeton University Press. (doi:10.1038/453034a)
13. Smith, M. J., Telfer, S., Kallio, E. R., Burthe, S., Cook, A. R., Lambin, X. & Begon, M. 2009 Host-pathogen time series data in wildlife support a transmission function between density and frequency dependence. *Proc. Natl. Acad. Sci.* **106**, 7905–7909. (doi:10.1073/pnas.0809145106)
14. Ryder, J. J., Miller, M. R., White, A., Knell, R. J. & Boots, M. 2007 Host-parasite population

- dynamics under combined frequency- and density-dependent transmission. *Oikos* **116**, 2017–2026. (doi:10.1111/j.2007.0030-1299.15863.x)
15. Knell, R. J., Begon, M. & Thompson, D. J. 1996 Transmission dynamics of *Bacillus thuringiensis* infecting *Plodia interpunctella*: a test of the mass action assumption with an insect pathogen. *Proc. R. Soc. B Biol. Sci.* **263**, 75–81. (doi:10.1098/rspb.1996.0013)
 16. Rachowicz, L. J. & Briggs, C. J. 2007 Quantifying the disease transmission function: effects of density on *Batrachochytrium dendrobatidis* transmission in the mountain yellow-legged frog *Rana muscosa*. *J. Anim. Ecol.* **76**, 711–721. (doi:10.1111/j.1365-2656.2007.01256.x)
 17. Goyens, J., Reijniers, J., Borremans, B. & Leirs, H. 2013 Density thresholds for Mopeia virus invasion and persistence in its host *Mastomys natalensis*. *J. Theor. Biol.* **317**, 55–61. (doi:10.1016/j.jtbi.2012.09.039)
 18. Ryder, J. J., Webberley, K. M., Boots, M. & Knell, R. J. 2005 Measuring the transmission dynamics of a sexually transmitted disease. *Proc. Natl. Acad. Sci.* **102**, 15140–15143. (doi:10.1073/pnas.0505139102)
 19. Luis, A. D., Douglass, R. J. D., Mills, J. N. M. & Bjørnstad, O. N. 2015 Environmental fluctuations lead to predictability in Sin Nombre hantavirus outbreaks. *Ecology* **96**, 1691–1701. (doi:10.1890/14-1910.1)
 20. Greer, A. L., Briggs, C. J. & Collins, J. P. 2008 Testing a key assumption of host-pathogen theory: density and disease transmission. *Oikos* **117**, 1667–1673. (doi:10.1111/j.1600-0706.2008.16783.x)
 21. Heesterbeek, J. A. & Metz, J. A. 1993 The saturating contact rate in marriage- and epidemic models. *J. Math. Biol.* **31**, 529–539. (doi:10.1007/bf00173891)
 22. Hu, H., Nigmatulina, K. & Eckhoff, P. 2013 The scaling of contact rates with population density for the infectious disease models. *Math. Biosci.* **244**, 125–134. (doi:10.1016/j.mbs.2013.04.013)
 23. Borremans, B., Reijniers, J., Hughes, N. K., Godfrey, S. S., Gryseels, S., Makundi, R. & Leirs, H. 2016 Nonlinear scaling of foraging contacts with rodent population density. *Oikos* **in press**. (doi:10.1111/oik.03623)
 24. Borremans, B., Vossen, R., Becker-Ziaja, B., Gryseels, S., Hughes, N., Van Gestel, M., Van Houtte, N., Günther, S. & Leirs, H. 2015 Shedding dynamics of Morogoro virus, an African arenavirus closely related to Lassa virus, in its natural reservoir host *Mastomys natalensis*.

- Sci. Rep.* **5**, 10445. (doi:10.1038/srep10445)
25. Katakweba, A., Mulungu, L., Eiseb, S., Mahlaba, T., Makundi, R., Massawe, A., Borremans, B. & Belmain, S. 2012 Prevalence of haemoparasites, leptospirae and coccobacilli with potential for human infection in the blood of rodents and shrews from selected localities in Tanzania, Namibia and Swaziland. *African Zool.* **47**, 119–127. (doi:10.3377/004.047.0112)
 26. Frame, J. D., Baldwin, J. M., Gocke, D. J. & Troup, J. M. 1970 Lassa fever, a new virus disease of man from West Africa. 1. Clinical description and pathological findings. *Am. J. Trop. Med. Hyg.* **19**, 670–676.
 27. Davis, D. H. 1953 Plague in Africa from 1935 to 1949; a survey of wild rodents in African territories. *Bull. World Health Organ.* **9**, 665–700.
 28. Gryseels, S., Rieger, T., Oestereich, L., Cuypers, B., Borremans, B., Makundi, R., Leirs, H., Günther, S. & Göy de Bellocq, J. 2015 Gairo virus, a novel arenavirus of the widespread *Mastomys natalensis*: Genetically divergent, but ecologically similar to Lassa and Morogoro viruses. *Virology* **476**, 249–256. (doi:10.1016/j.virol.2014.12.011)
 29. Göy De Bellocq, J., Borremans, B., Katakweba, A., Makundi, R., Baird, S. J. E., Becker-Ziaja, B., Günther, S. & Leirs, H. 2010 Sympatric Occurrence of 3 Arenaviruses, Tanzania. *Emerg. Infect. Dis.* **16**, 10–13. (doi:10.3201/eid1604.091721)
 30. Leirs, H., Stenseth, N. C., Nichols, J. D., Hines, J. E., Verhagen, R. & Verheyen, W. 1997 Stochastic seasonality and nonlinear density-dependent factors regulate population size in an African rodent. *Nature* **389**, 176–180. (doi:10.1038/38271)
 31. Sluydts, V., Davis, S., Mercelis, S. & Leirs, H. 2009 Comparison of multimammate mouse (*Mastomys natalensis*) demography in monoculture and mosaic agricultural habitat: Implications for pest management. *Crop Prot.* **28**, 647–654. (doi:10.1016/j.cropro.2009.03.018)
 32. Borremans, B., Leirs, H., Gryseels, S., Günther, S., Makundi, R. & de Bellocq, J. G. 2011 Presence of Mopeia virus, an African arenavirus, related to biotope and individual rodent host characteristics: implications for virus transmission. *Vector-Borne Zoonotic Dis.* **11**, 1125–1131. (doi:10.1089/vbz.2010.0010)
 33. Peel, A. J., Pulliam, J. R. C., Luis, A. D., Plowright, R. K., Shea, T. J. O., Hayman, D. T. S., Wood, J. L. N., Webb, C. T. & Restif, O. 2014 The effect of seasonal birth pulses on pathogen persistence in wild mammal populations. *Proc. R. Soc. B Biol. Sci.* **281**, 20132962. (doi:10.1098/rspb.2013.2962)

34. Ross, R. 1916 An application of the theory of probabilities to the study of a priori pathometry - part I. *Proc. R. Soc. A* **92**, 204–230. (doi:10.1098/rspa.1916.0007)
35. Kermack, W. O. & McKendrick, A. G. 1927 A contribution to the mathematical theory of epidemics. *Proc. R. Soc. London Ser. A* **115**, 700–721.
36. Cao, Y., Gillespie, D. T. & Petzold, L. R. 2007 Adaptive explicit-implicit tau-leaping method with automatic tau selection. *J. Chem. Phys.* **126**. (doi:10.1063/1.2745299)
37. de Jong, M. C. M. M., Bouma, A., Diekmann, O. & Heesterbeek, H. 2002 Modelling transmission: mass action and beyond. *Trends Ecol. Evol.* **17**, 5347–5347. (doi:10.1016/S0169-5347(01)02398-9)
38. Vander Wal, E., Yip, H. & McLoughlin, P. D. 2012 Sex-based differences in density-dependent sociality: an experiment with a gregarious ungulate. *Ecology* **93**, 206–212. (doi:10.1890/11-0020.1)
39. Ramsey, D., Spencer, N., Caley, P., Efford, M., Hansen, K., Lam, M. & Cooper, D. 2002 The effects of reducing population density on contact rates between brushtail possums: implications for transmission of bovine tuberculosis. *J. Appl. Ecol.* **39**, 806–818. (doi:10.1046/j.1365-2664.2002.00760.x)
40. Cross, P., Creech, T., Ebinger, M. & Manlove, K. 2013 Female elk contacts are neither frequency nor density dependent. *Ecology* **94**, 2076–2086. (doi:10.1890/12-2086.1)
41. Borremans, B., Hughes, N. K., Reijniers, J., Sluydts, V., Katakweba, A. A. S., Mulungu, L. S., Sabuni, C. A., Makundi, R. H. & Leirs, H. 2014 Happily together forever: temporal variation in spatial patterns and complete lack of territoriality in a promiscuous rodent. *Popul. Ecol.* **56**, 109–118. (doi:10.1007/s10144-013-0393-2)
42. Ostfeld, R. S. & Canham, C. D. 1995 Density-dependent processes in meadow voles: an experimental approach. *Ecology* **76**, 521–532. (doi:10.2307/1941210)

Figures

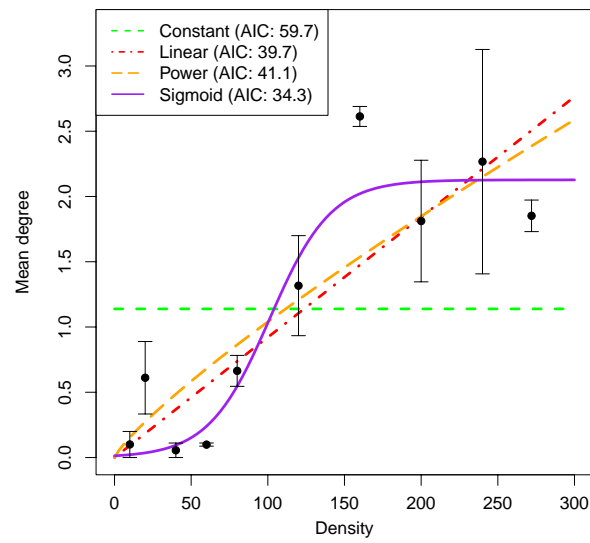


Figure 1. Contact-density functions fitted to experimental data from Borremans *et al.* [23], showing mean degree (the number of individuals one focus individual contacted) for a range of population densities (number of animals per ha = $\frac{N}{A}$).

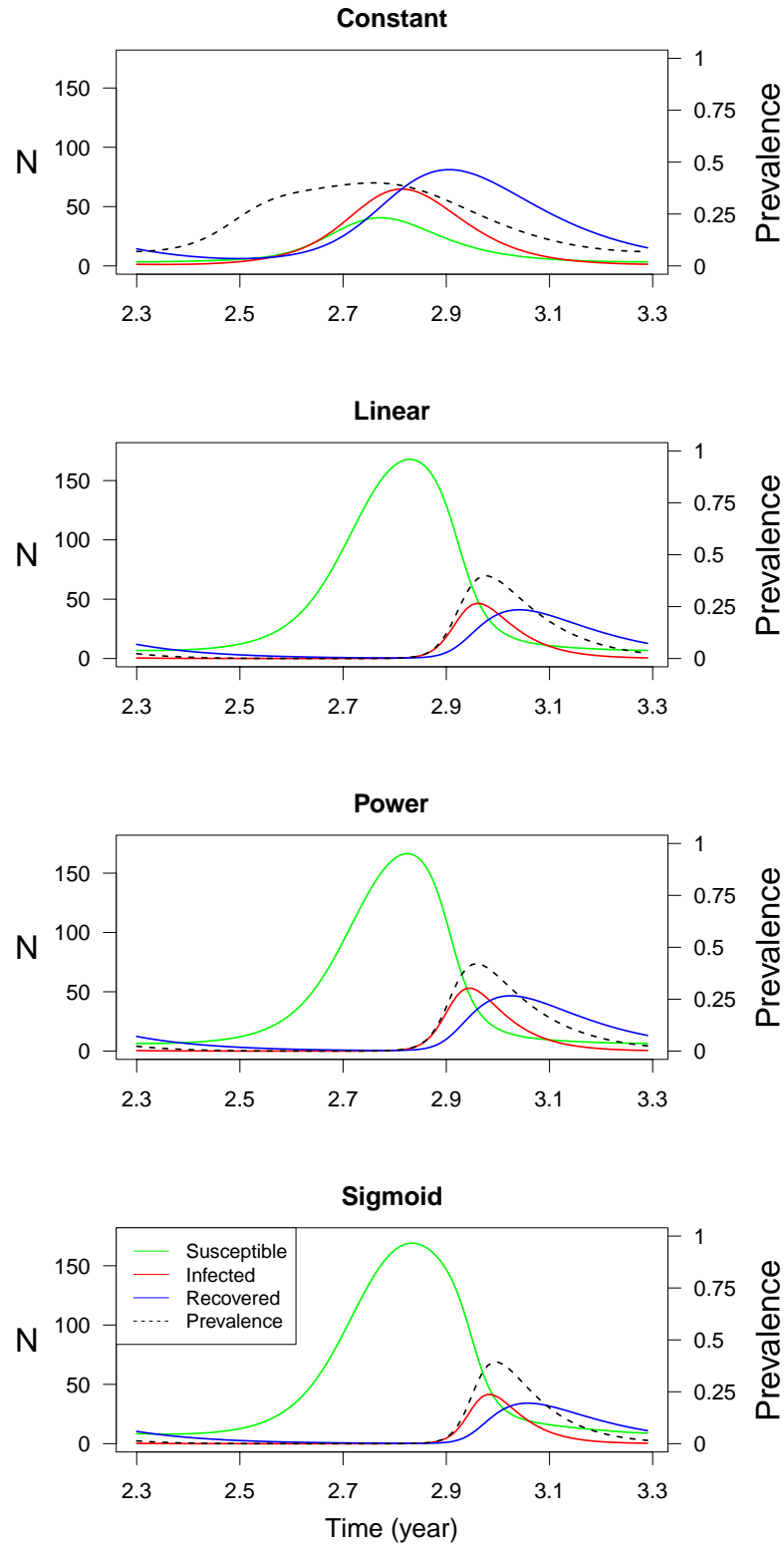


Figure 2. Output of the deterministic models, using four different contact-density functions. Infectious period $\frac{1}{\gamma} = 30$ days, transmission rate $p = 50$, initial population size $N_0 = 100$.

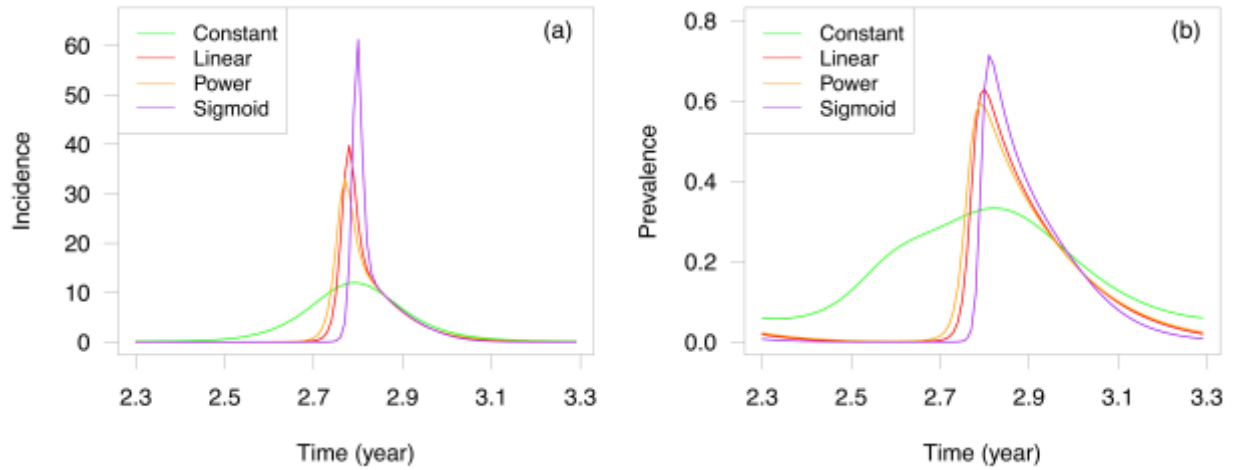


Figure 3. Incidence (a) and prevalence (b) for the different contact-density functions, during one year.

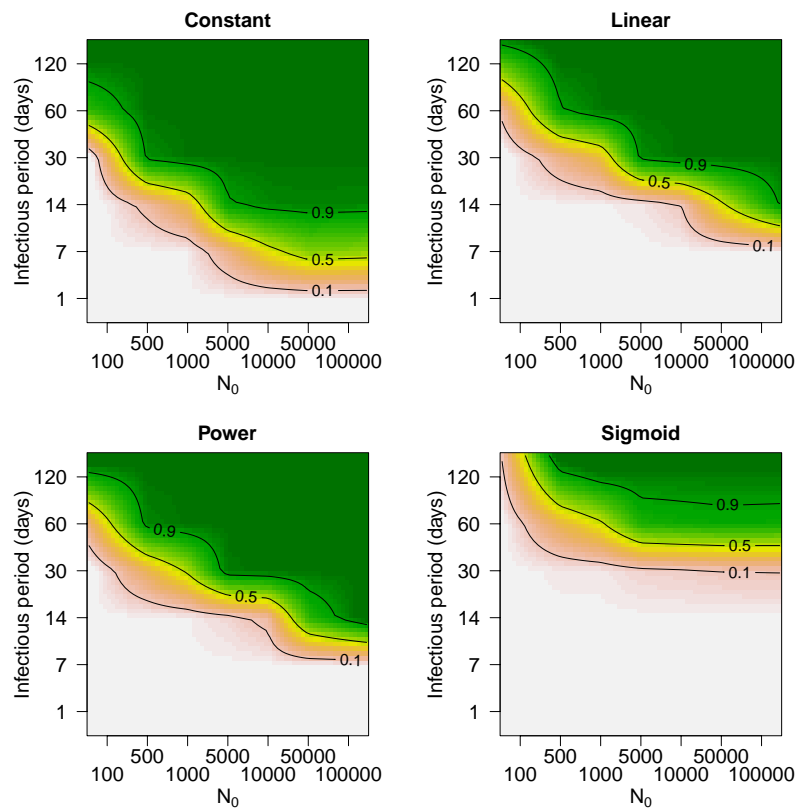


Figure 4. Invasion probabilities for the different contact-density functions, for a range of infectious periods $\frac{1}{\gamma}$ and initial population sizes N_0 (transmission rate $p = 50$). Simulations were conducted for all values indicated by tick marks on the axes, and results are interpolated between these values for illustration.

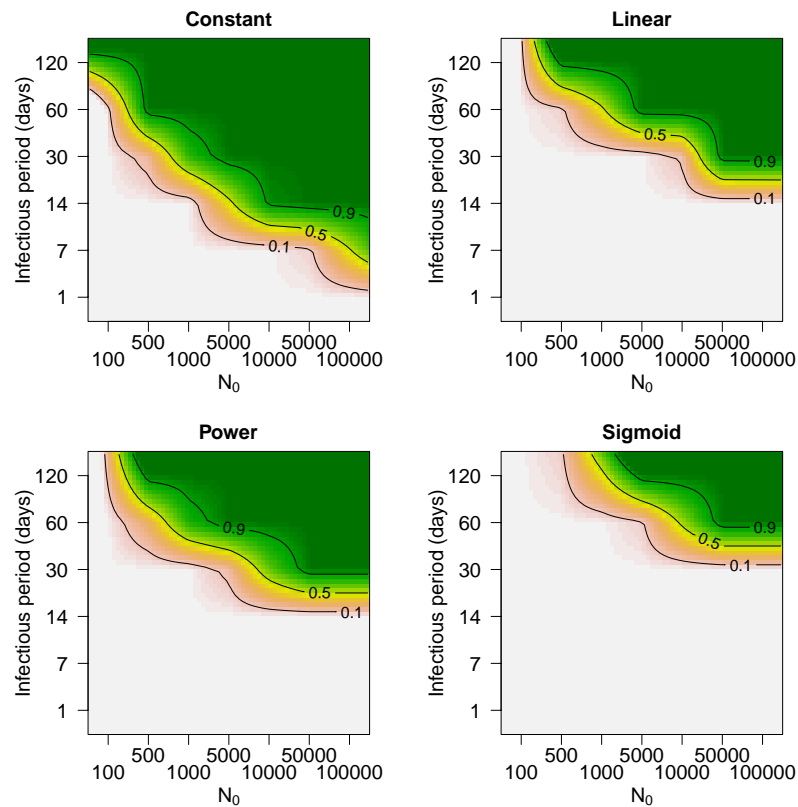


Figure 5. Persistence probabilities for the different contact-density functions, for a range of infectious periods $\frac{1}{\gamma}$ and initial population sizes N_0 (transmission rate $p = 50$). Simulations were conducted for all values indicated by tick marks on the axes, and results are interpolated between these values for illustration.